Journal of Engineering and Applied Sciences 6 (1): 27-37, 2011
ISSN: 1816-949X

The Effect of Nickel Micro Powder Suspended Dielectric on EDM Performance Measures of EN-19 Steel

[1]Kuldeep Ojha, [1]R.K. Garg and [2]K.K. Singh
[1]Department of Industrial and Production Engineering,
B.R. Ambedkar National Institute of Technology, 144011 Jalandhar, Punjab, India
[2]Department of Mechanical Engineering and Mining Machinery Engineering,
Indian School of Mines (ISM), 826004 Dhanbad, Jharkhand, India

Abatract: In this study, a Material Removal Rate (MRR), Tool Wear Rate (TWR) and Surface Roughness (SR) study on the Powder Mixed Electrical Discharge Machining (PMEDM) of EN-19 (AISI-4140) steel has been carried out. Response Surface Methodology (RSM) has been used to plan and analyze the experiments. Peak current, pulse on time, diameter of electrode and concentration of micro-nickel powder added into dielectric fluid of EDM were chosen as process parameters to study the PMEDM performance in terms of MRR, TWR and SR. Experiments have been performed on newly designed experimental setup developed in laboratory. Most important parameters affecting selected performance measures have been identified and optimum process conditions have been found. Also recommended optimal conditions have been verified by conducting confirmation experiments.

Key words: Material removal rate, tool wear rate, surface roughness, performance, parameters, laboratory

INTRODUCTION

Electrical discharge machining is an important manufacturing process for tool mould and die industries. This process is finding an increasing application for because of its ability to produce geometrically complex shapes and its ability to machine materials irrespective to their hardness. However, poor surface finish and low machining efficiency limits its further applications (Zhao *et al*., 2002). Powder Mixed Electrical Discharge Machining (PMEDM) is a relatively new material removal process applied to improve the machining efficiency and surface finish in presence of powder mixed dielectric fluid (Zhao *et al*., 2002; Kansal *et al*., 2003).

Researchers have explained the working principle of powder mixed electrical discharge machining process (Zhao *et al*., 2002; Kansal *et al*., 2005). When a voltage is applied between the electrode and the work piece facing each other with a gap, an electric field in the range of 10^5-10^7 V m^{-1} is created. The powder particles in the spark gap get energized. These charged particles are accelerated by the developed electric field and act as conductors. The conductive particles promote breakdown in the gap and also increase the spark gap between tool and the workpiece. Under the sparking area, the particles come closer and arrange themselves in chain like structures between both the electrodes. The interlocking between the different powder particles takes place in the direction of current flow. This chain formation helps in bridging the discharge gap between electrodes and also results in decreasing the insulating strength of the dielectric fluid. The easy short circuit takes place, causing early explosion in the gap resulting in series discharges under the electrode area.

The faster sparking within a discharge occur causing faster erosion from the workpiece surface and hence, the Material Removal Rate (MRR) increases. At the same time, the added powder also modifies the plasma channel making it enlarged and widened. The sparking is uniformly distributed among the powder particles hence, electric density of the spark decreases. Due to uniform distribution of sparking among the powder particles, shallow craters are produced on the workpiece surface resulting in improvement in surface finish.

Literature review: Erden and Bilgin (1980) has investigated the effect of abrasive powder mixed into the dielectric fluid and proposed that the machining rate increased with an increase of the powder concentration due to decreasing the time lag. Jeswani (1981) have investigated the effect of addition of graphite powder to kerosene and proposed that the material removal

Corresponding Author: Kuldeep Ojha, Department of Industrial and Production Engineering,
B.R. Ambedkar National Institute of Technology, 144011 Jalandhar, Punjab, India

rate was improved around 60% and electrode wear ratio was reduced about 15% by using the kerosene oil mixed with 4 g L^{-1} graphite powder. Mohri *et al.* (1985, 1988, 1991), Yan and Chen (1993, 1994a, b), Yan *et al.* (2004) and Uno and Okada (1997) have investigated the influence of silicon powder addition on machining rate and surface roughness in EDM. Wong *et al.* (1998), Furutani *et al.* (2001) and Yan *et al.* (2004) have proposed that the machined surface properties including hardness, wear resistance and corrosion resistance could be significantly improved by using the PMEDM process. Wu *et al.* (2005) have discussed the improvement of the machined surface by adding aluminum powder and surfactant into dielectric fluid. Narumiya *et al.* (1989) concluded that Al and Si powders yield better surface finish under specific work conditions.

Kobayashi *et al.* (1992) investigated the effects of suspended powder in dielectric fluid on MRR and SR of SKD-61 material. Uno *et al.* (1998) have studied the effect of nickel powder mixed working fluid modifies the surface of aluminum bronze components. Okada *et al.* (2000) have proposed a new method for forming hard layer containing titanium carbide by EDM with carbon powder mixed fluid using titanium electrode. Chow *et al.* (2000) have studied the EDM process by adding SiC and aluminum powders into kerosene for the micro-slit machining of titanium alloy. Wang have investigated the effect of Al and Cr powder mixture in kerosene. Tzeng and Lee (2001) have reported the effect of various powder characteristics on EDM of SKD-11 material. Furutani and Shiraki (2002) have proposed a deposition method of lubricant layer during finishing EDM process to produce parts for ultra high vacuum.

Simao *et al.* (2003) have explored the role of PMEDM in modifying the surface properties of the workpiece by application of Taguchi method. Pecas and Henriques (2003) have investigated the influence of silicon powder mixed dielectric on conventional EDM. The relationship between the roughness and pulse energy was roughly investigated under a few sets of the conditions in the removal process. However, the effect of the energy was not systematically analyzed. Cogun *et al.* (2006) have made an experimental investigation on the effect of powder mixed dielectric on machining performance. Kansal *et al.* (2007) have studied the effect of silicon powder mixed EDM on machining Rate of AISI D2 Die steel.

Kansal *et al.* (2005) worked to optimize the process parameters of PMEDM by using the response surface methodology. Pecas and Henriques (2008a, b) have investigated the effect of the electrode area in the surface roughness and topography and also the influence of the powder concentration and dielectric flow in the surface morphology. Prihandana *et al.* (2009) have investigated the effect of micro-powder suspension and ultrasonic vibration of dielectric fluid in micro-EDM processes by applying the Taguchi approach. Furutani *et al.* (2009) have investigated the influence of electrical conditions on performance of electrical discharge machining with powder suspended in working oil for titanium carbide deposition process.

Kung *et al.* (2009) have studied the influence of MRR and electrode wear ratio in the PMEDM of cobalt-bonded tungsten carbide. Elaborate scrutiny of the literature reveals that material removal mechanism of PMEDM process is very complex and theoretical modeling of the process is very difficult. Regarding empirical results, much research is required with more work-tool-powder-parametric combinations to make the process commercially applicable. Also, most of the research is with Al, Si and graphite powders. Much investigation is needed regarding other types of powder like Cr, Ni, Mo, etc.

In present research, different parametric combinations of peak current, duty cycle, electrode diameter and powder concentration of micro-Ni Powder in dielectric has been explored for EN-19 steel. Literature review reveals that this combination has not been explored yet. EN-19 steel finds wide applications in industry in making components of mediums and large cross section, requiring high tensile strength and toughness for automatic engineering and gear and engine construction such as crane shafts steering, connecting rods. Investigation of EN-19 steel with promising emerging area of PMEDM is useful in research field.

MATERIALS AND METHODS

Experimental set-up: Figure 1 shows line diagram of experimental setup used for experimentation. The experiments have been performed on T-3822 EDM machine manufactured by electronica. The points considered in designing PMEDM set-up are:

- The powder should not enter the main dielectric tank to avoid filtering of powder particles
- The dielectric should be continuously stirred or circulated to prevent settling of the powder and to maintain uniform concentration

The main dielectric sump has been disconnected from dielectric tank by valve arrangements. To obtain even and homogeneous distribution of powder particles in suspended form in dielectric, a flush mixing was provided

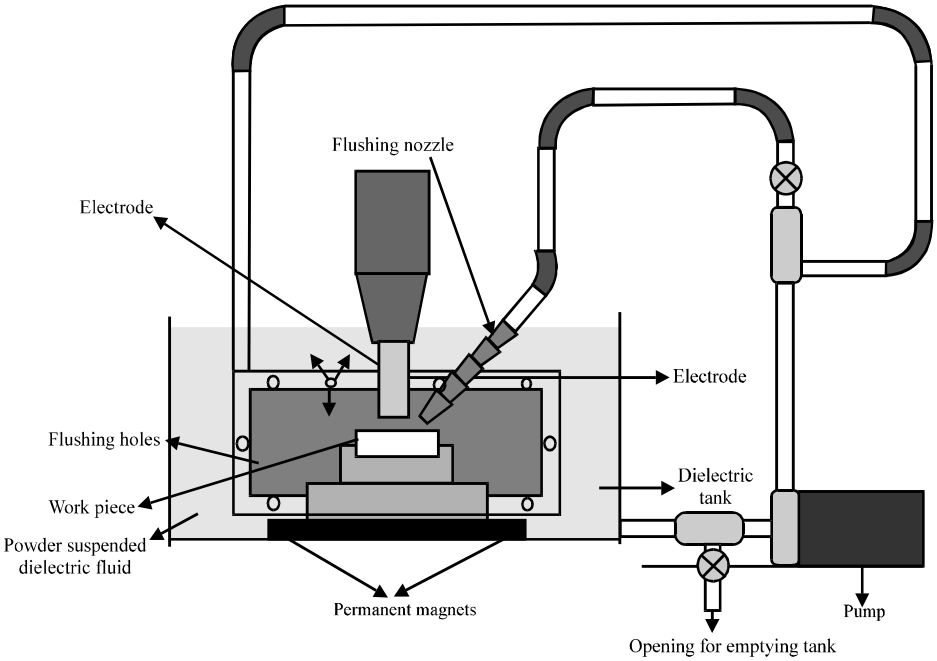

Fig. 1: Line diagram of experimental setup

Table 1: Chemical composition of steel EN-19

C (%)	Si (%)	Mn (%)	Cr (%)	Mo (%)	Iron
0.37	0.37	0.57	1.1	0.24	Rest

Table 2: Specifications of EN-19 work piece material

Hardening temp.	Quenching medium	Tempering temperature	Japan JIS	AISI no.
900-950	Oil	200-225	SCM-4	4140

Table 3: Specifications of kerosene oil

Dielectric constant	Electrical conductivity	Dynamic Density	viscosity	AISI no.
1.8	1.6×10^{-14} S m^{-1}	730	0.94 m Pas	4140

in the tank by means of 25 mm diameter plastic pipe with 3 mm diameter holes in it. The dielectric was sucked from bottom level of tank by means of a pump (power 1.5 W and maximum discharge 5500 LPH) and was pumped into plastic pipe frame. The output from pump is divided into two parts and from one part flushing nozzle is connected. Flow through flushing nozzle is adjusted to 500 L h^{-1} through 4 mm opening nozzle by adjusting valve opening.

The work piece material used in this study is EN-19 steel (AISI-4140). The chemical composition of steel as determined by optical emission spectrophotometer analysis is shown in Table 1. Other specifications of material given by manufacturer are shown in Table 2.

Commercial copper with 99% purity (having electrical conductivity 5.69×10^{7} S M^{-1}) has been applied as tool electrode. By spectrophotometer analysis the composition of electrode material has been determined. Commercial kerosene has been used as dielectric fluid. The specifications have been shown in Table 3. Also, the properties of micro Ni-powder suspended in dielectric have been shown in Table 4.

Experimental settings: Following experimental settings has been applied in this study.

Design of experiments

Selection of design factors: The status of nickel powder particles mixed into the dielectric fluid has a significant role in determining and evaluating the EDM characteristics of a product. There are many design factors to be considered concerning the effects of nickel powder particles but in this study concentration of suspended powder particles has been taken as variable. In addition, the discharge current (I_P, A) and pulse on time (τ_P, μs) were only taken into account as design factors. The reason why these two factors have been chosen is that they are the most general and frequently used among EDM researchers (Kung *et al*., 2009). Electrode diameter has also been selected as design factor as electrode shape parameter.

Selection of response variables: The response variables selected in this study were MRR, TWR and the Surface Roughness (SR). Both MRR and TWR refer to the machining efficiency of the PMEDM process and the wear of copper electrode, respectively and are defined as

Table 4: Specifications of Ni-powder used

Particle size	Ni (%)	Particle shape	H_2 loss (%)	Apparent density	Flow rate	Electricalconductivity
1-2 μm	99.9	Spherical	0.52	3.96 g cc^{-1}	25 sec to flow 50 g	14.3×10^6 S m^{-1}

follows: MRR (mm^3 min^{-1}) = (Wear weight of work piece)/(time of machining x density of work piece material) TWR (mm^3 min^{-1}) = (Wear weight of tool electrode)/(time of machining x density of electrode material). The work piece and electrode were weighed before and after each experiment using an electric balance with a resolution of 0.001 mg to determine the value of MRR and TWR. For efficient evaluation of the PMEDM process, the larger MRR and the smaller TWR are regarded as the best machining performance. Therefore, the MRR is considered as the larger the better characteristic and the TWR is considered as the smaller-the-better characteristic in this experimentation.

SR has been measured in terms of arithmetic mean (R_a) which is defined as arithmetic average roughness of deviations of roughness profile from the central line along the measurement.

Experimental design: Response Surface Methodology (RSM) is used in design matrix formation which is an empirical modeling approach using polynomials as the local approximations to obtain true input/output relationships (Montgomery, 1997). The experimental plans were designed on the basis of the Central Composite Design (CCD) technique of RSM. The factorial portion of CCD is a full factorial design with all combinations of the factors at two levels (high, +1 and low, -1) and composed of the 8 star points and 7 central points (coded level 0). Central points are the midpoint between the high and low levels. The star points are at the face of the cube portion on the design that corresponds to an $\alpha = 1$ and this type of design is commonly called the face-centered CCD. In this study, the experimental plan was conducted using the stipulated conditions according to the face-centered CCD and involved a total of 31 experimental observations at 4 independent input variables (Table 5).

The machining time for each experimental specimen is 15 min. This was set up before the operation of the machine reached the stable state. The levels of design factors have been selected in accordance with literature consulted as well as by personal experience. The design factors selected for study with their low and high levels are shown in Table 6.

Design expert 8.0.4 software was used for design of experiments and regression and graphical analysis of data obtained. The optimum conditions have been obtained by solving the regression equations and by analyzing response surface contours.

Table 5: Experimental settings

Polarity	Supply volt	Dielectric flow rate	Power factor	Machining time
Positive	415, 3 phase, 50 Hz	500 L h^{-1}	0.3	15 min

Table 6: Process parameters and their levels

	Notation			Range and levels		
Parameters	Natural	Coded	Unit	-1	0	+1
Current	I	X_1	A	4	6	8
Duty cycle (%)	D(%)	X_2	%	54	63	72
Powder concentration	C	X_3	g L^{-1}	2	4	6
Tool diameter	D	X_4	mm	8	12	16

Response surface modeling: As stated earlier, Response surface methodology has been applied for modeling and analysis of parameters. The quantitative relationship between desired responses and independent process variables can be represented as:

$$Y = f(X_1, X_2, X_3, ... X_n)$$

Where:

Y = The desired response
f = The response function
X_1, X_2 = Independent parameters

By plotting the expected responses, a surface known as response surface is obtained. RSM aims at approximating f by using the fitted second order Polynomial regression model which is called the quadratic model. The model can be represented as follows:

$$Y = C_0 + \sum_{i=1}^{5} C_i X_n + \sum_{i=1}^{5} d_i X_i^2 \pm \epsilon$$

RESULTS AND DISCUSSION

About 30 experimental runs have been conducted and values of MRR, TWR and SR along with design matrix are shown in Table 7 to avoid any systematic error creeping into system. Analysis of Variance (ANOVA) is performed on collected data for testing significance of regression model and model coefficients.

Analysis of MRR: The fit summery table formed recommended quadratic model as statically significant for MRR analysis. The results of quadratic model in form of ANOVA are shown in Table 8. The model F-value of 7.91 implies the model is significant. There is only a 0.01%

Table 7: Experimental design matrix and collected data

	Coded values				Natural values				Responses	
Run no.	X_1	X_2	X_3	X_4	I (A)	D (%)	C (g L^{-1})	D (mm)	MRR (mm^3 min^{-1})	TWR (mm^3 min^{-1})
1	0	0	0	0	6	63	4	12	7.01	0.032
2	+1	0	0	0	8	63	4	12	8.13	0.048
3	0	0	0	+1	6	63	4	16	5.49	0.036
4	-1	-1	-1	-1	4	54	2	8	2.43	0.023
5	0	0	0	0	6	63	4	12	6.73	0.030
6	0	0	-1	0	6	63	2	12	5.12	0.028
7	-1	0	0	0	4	63	4	12	5.04	0.017
8	+1	+1	-1	+1	8	72	2	16	6.85	0.035
9	+1	+1	-1	-1	8	72	2	8	4.65	0.045
10	0	0	0	0	6	63	4	12	7.87	0.035
11	+1	+1	+1	+1	8	72	6	16	6.93	0.036
12	+1	-1	-1	+1	8	54	2	16	6.86	0.035
13	-1	-1	+1	+1	4	54	6	16	3.41	0.027
14	-1	-1	-1	+1	4	54	2	16	1.76	0.025
15	+1	-1	-1	-1	8	54	2	8	5.84	0.034
16	+1	+1	+1	-1	8	72	6	8	8.01	0.036
17	0	0	0	0	6	63	4	12	6.61	0.034
18	+1	-1	+1	-1	8	54	6	8	6.83	0.032
19	+1	-1	+1	+1	8	54	6	16	5.81	0.035
20	0	-1	-1	0	6	54	4	12	5.56	0.038
21	0	+1	-1	0	6	72	4	12	5.68	0.028
22	-1	+1	-1	-1	4	72	2	8	2.37	0.016
23	-1	+1	+1	+1	4	72	6	16	2.45	0.019
24	0	0	+1	+1	6	63	6	12	5.05	0.027
25	-1	+1	+1	-1	4	72	6	8	3.01	0.013
26	0	0	0	0	6	63	4	12	6.62	0.036
27	-1	-1	+1	-1	4	54	6	8	3.45	0.018
28	0	0	0	0	6	63	4	12	5.59	0.036
29	0	0	0	-1	6	63	4	8	3.43	0.031
30	-1	+1	-1	+1	4	72	2	16	2.97	0.015

Table 8: ANOVA table for MRR (before backward elimination)

Sources	Sum of squares	df	Mean square	F-value	Prob>F	p value
Model	88.31	14	6.3070	7.914	0.0001	Significant
A-current	60.57	1	60.5730	76.010	<0.0001	
B-duty cycle (%)	0.052	1	0.0522	0.066	0.8013	
C-powder concentration	2.067	1	2.0670	2.594	0.1281	
D-tool diameter	0.350	1	0.3500	0.439	0.5176	
AB	0.114	1	0.1130	0.143	0.7107	
AC	0.022	1	0.0210	0.027	0.8710	
AD	0.200	1	0.2000	0.251	0.6235	
BC	0.056	1	0.0560	0.071	0.7938	
BD	0.219	1	0.2180	0.274	0.6082	
CD	2.139	1	2.1380	2.684	0.1222	
A^2	1.297	1	1.2970	1.628	0.2215	
B^2	0.172	1	0.1710	0.215	0.6492	
C^2	1.627	1	1.6270	2.042	0.1735	
D^2	5.206	1	5.2050	6.532	0.0219	
Residual	11.95	15	0.7960	-	-	
Lack of fit	9.251	10	0.9250	1.711	0.2878	Non-significant
Pure error	2.704	5	0.5400	-	-	
Cor total	100.3	29	-	-	-	

Std. Dev = 0.89; R^2 = 0.8808; Mean = 5.25; Adj R^2 = 0.7695; C.V. % = 17.00; Pred R^2 = 0.4253; PRESS = 57.62 and Adeq precision = 11.150

chance that a model F-value this large could occur due to noise. Values of Prob>F >0.0500 indicate model terms are significant. In this case A (current), D2 are significant model terms. Values >0.1000 indicate the model terms are not significant. The result shows that the current is most significant factor affecting the MRR.

The lack of fit F-value of 1.71 implies the lack of fit is not significant relative to the pure error. There is a 28.78% chance that a lack of fit F-value this large could occur due to noise. Non-significant lack of fit is good, we want the model to fit. The Pred R^2 of 0.4253 is not as close to the Adj R^2 of 0.7695 as 1 might normally expect. This may indicate a large block effect or a possible problem with the model and/or data. Adeq precision measures the signal to noise ratio. A ratio <4 is desirable. Model ratio of 11.150 indicates an adequate

Table 9: ANOVA table for MRR (after backward elimination)

Sources	Sum of squares	df	Mean square	F-value	P>F	p value
Model	85.0830	5	17.016	26.910	<0.0001	Significant
A-current	60.5730	1	60.573	95.790	<0.0001	
C-powder concentration	2.0672	1	2.067	3.269	0.0831	
D-tool diameter	0.3500	1	0.350	0.553	0.4641	
CD	2.1389	1	2.138	3.382	0.0783	
D^2	19.9530	1	19.953	31.550	<0.0001	
Residual	15.1770	24	0.632	-	-	
Lack of fit	12.4730	19	0.656	1.214	0.4519	Non-significant
Pure error	2.7037	5	0.540	-	-	

Std. Dev = 0.80; R^2 = 0.8486; Mean = 5.25; Adj R^2 = 0.8171; C.V(%) = 15.14; Pred R^2 = 0.7733; PRESS = 22.72 and Adeq precision = 17.371

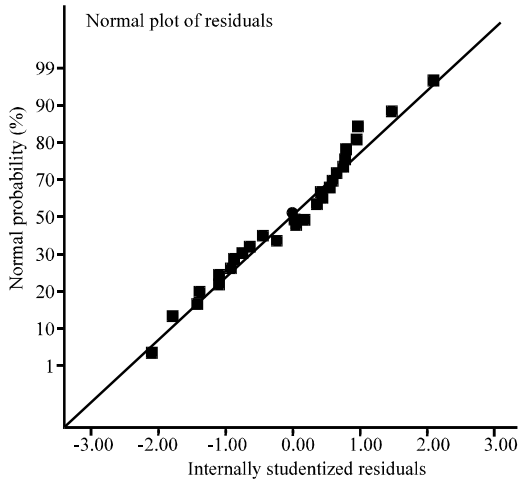

Fig. 2: Normal probability plot residuals for MRR

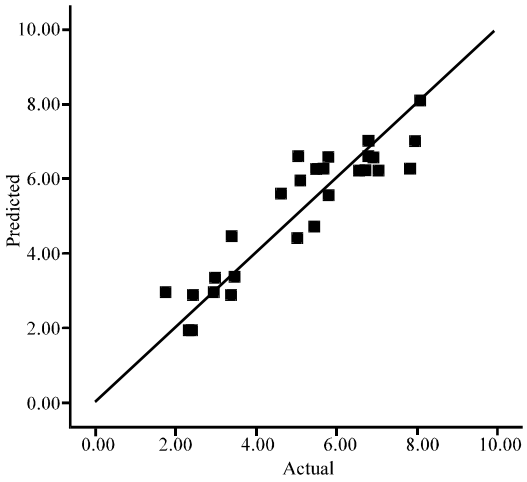

Fig. 3: Plot of actual vs. predicted response of MRR data

signal. This model can be used to navigate the design space. If there are many insignificant model terms (not counting those required to support hierarchy), model reduction may improve the model. To fit the quadratic model for MRR appropriate, the non significant terms are eliminated by backward elimination process. The ANOVA table for the reduced quadratic model for MRR is shown in Table 9. The model F-value of 26.91 implies the model is significant. There is only 0.01% chance that a model F-value this large could occur due to noise. Values of Prob>F>0.0500 indicate model terms are significant. In this case A, D^2 are significant model terms. Values <0.1000 indicate the model terms are not significant. If there are many insignificant model terms (not counting those required to support hierarchy), model reduction may improve the model.

The lack of fit F-value of 1.21 implies the lack of fit is not significant relative to the pure error. There is a 45.19% chance that a lack of fit F-value this large could occur due to noise. Non-significant lack of fit is good we want the model to fit. The Pred R^2 of 0.7733 is in reasonable agreement with the Adj R^2 of 0.8171. Adeq precision measures the signal to noise ratio. A ratio <4 is desirable. The ratio of 17.371 indicates an adequate signal. This model can be used to navigate the design space.

It is noticed that the residuals are falling on a straight line which means that the errors are normally distributed as shown in Fig. 2. Further each observed value is compared with the predicted value calculated from the shown in Fig. 3. The plot is randomly scattered (constant range of residuals across the graph) as desired.

Thus, the regression model is fairly well fitted with the observed values. After eliminating the non-significant terms, the final response equation for MRR is given as follows: final equation in terms of coded factors: final equation in terms of coded factors: MRR = +6.25+1.83 A+0.34 C+0.14 D-0.37 CD - 1.66 D^2. Final equation in terms of actual factors: MRR = -17.52486+0.91722× Current+ 0.71788× Powder concentration +2.71476× Tool diameter- 0.045703× Powder concentration x Tool diameter -0.10405× Tool diameter^2. Figure 4-6 shows the estimated response surface for MRR in relation to the design parameters of peak current with tool diameter, powder concentration and duty cycle.

As shown in Fig. 4-6, the MRR tends to increase, considerably with increase in current for any value of other factors. Hence, maximum MRR is obtained at high current. The MRR increases with increase in tool diameter owing to increase in current. After certain level of range of 12 mm, the MRR tends to decrease due to

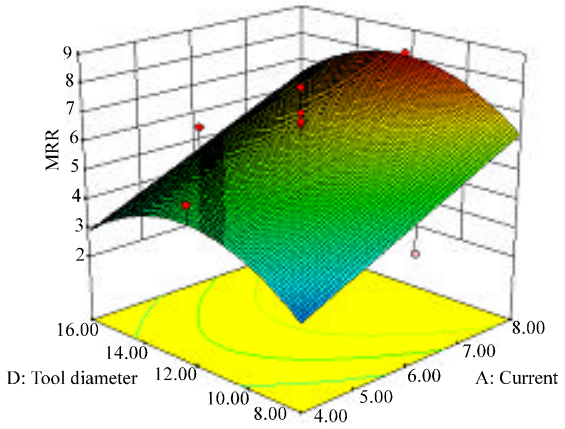

Fig. 4: Response surface for MRR showing effect of current and tool diameter

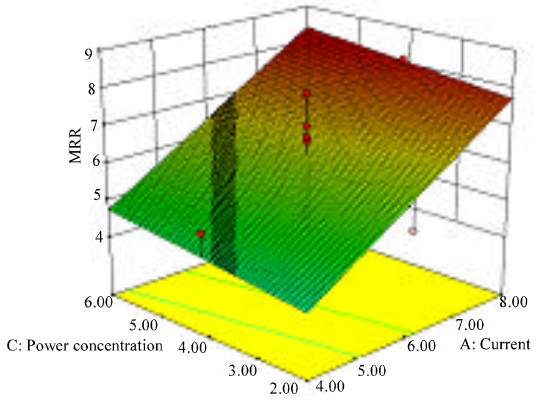

Fig. 5: Response surface for MRR showing effect of current and powder concentration

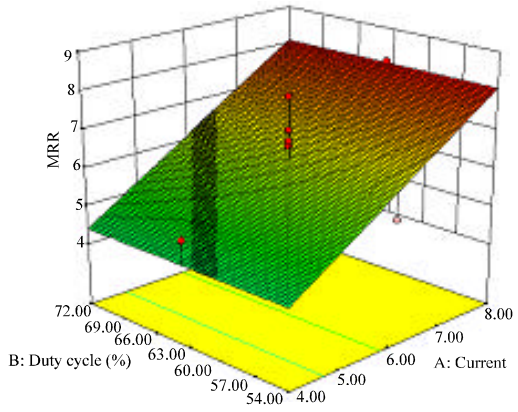

Fig. 6: Response surface for MRR showing effect of current and duty cycle

inefficient flushing. MRR is found to increase with duty cycle and powder concentration but there effect is not so, significant.

Analysis of TWR: The fit summery table formed for TWR recommends quadratic model as statically significant analysis. The results of quadratic model in form of ANOVA are shown in Table 10. The model F-value of 11.93 implies the model is significant. There is only a 0.01% chance that a model F-value this large could occur due to noise. Values of Prob>F>0.0500 indicate model terms are significant. In this case A, AB, C^2 are significant model terms. Values <0.1000 indicate the model terms are not significant.

The lack of fit F-value of 2.61 implies the lack of fit is not significant relative to the pure error. There is a 15.03% chance that a lack of fit F-value this large could occur due to noise. Non-significant lack of fit is good as we want the model to fit. The Pred R^2 of 0.6508 is in reasonable agreement with the Adj R^2 of 0.8407. Adeq precision measures the signal to noise ratio. A ratio <4 is desirable. The ratio of 12.900 indicates an adequate signal. This model can be used to navigate the design space.

Again if there are many insignificant model terms, model reduction may improve the model. To fit the quadratic model for TWR appropriate, the non significant terms are eliminated by backward elimination process. The ANOVA table for the reduced quadratic model for MRR is shown in Table 11.

The final TWR model F-value of 24.62 implies the model is significant. There is only a 0.01% chance that a model F-value this large could occur due to noise. Values of Prob>F>0.0500 indicate model terms are significant. In this case A, AB, C^2 are significant model terms. Values <0.1000 indicate the model terms are not significant. If there are many insignificant model terms (not counting those required to support hierarchy), model reduction may improve your model. The lack of fit F-value of 1.96 implies the lack of fit is not significant relative to the pure error. There is a 23.51% chance that a lack of fit F-value this large could occur due to noise. Non-significant lack of fit is good since, we want the model to fit. The Pred R^2 of 0.8109 is in reasonable agreement with the Adj R^2 of 0.8670. Adeq precision measures the signal to noise ratio. A ratio <4 is desirable. The ratio of 18.811 indicates an adequate signal. The model for TWR can be used to navigate the design space.

It is again noticed that the residuals are falling on a straight line for same model which means that the errors are normally distributed as shown in Fig. 7. Further each observed value is compared with the predicted value calculated from the model shown in Fig. 8. The plot is randomly scattered as desired. Thus the regression model is fairly well fitted with the observed values. After eliminating the non-significant terms, the final response equation for MRR is given as follows:

Table 10: ANOVA table for TRR (before backward elimination)

Sources	Sum of squares	df	Mean square	F-value	Prob>F	p value
Model	0.002	14	0.000142749	11.93	<0.0001	Significant
A-current	0.0015	1	0.001476056	123.3	<0.0001	
B-duty cycle (%)	3E-05	1	0.000032	2.674	0.1228	
C-powder concentration	9E-06	1	9.38889E-06	0.785	0.3897	
D-tool diameter	1E-05	1	0.0000125	1.045	0.3230	
AB	0.0001	1	0.00013225	11.05	0.0046	
AC	4E-06	1	4E-06	0.334	0.5718	
AD	3E-05	1	0.00003025	2.528	0.1327	
BC	3E-07	1	2.5E-07	0.021	0.8870	
BD	3E-05	1	0.000025	2.089	0.1689	
CD	4E-05	1	0.00004225	3.53	0.0798	
A^2	8E-07	1	8.16587E-07	0.068	0.7975	
B^2	1E-08	1	9.76874E-09	8E-04	0.9776	
C^2	8E-05	1	8.01348E-05	6.696	0.0206	
D^2	5E-07	1	4.98405E-07	0.042	0.8410	
Residual	0.0002	15	1.19674E-05	-	-	
Lack of fit	0.0002	10	1.50678E-05	2.613	0.1503	Non-significant
Pure error	3E-05	5	5.76667E-06	-	-	
Cor total	0.0022	29	-	-	-	

Std. dev = 3.459E-003; R^2 = 0.9176; Mean = 0.030; Adj R^2 = 0.8407; C.V(%) = 11.53; Pred R^2 = 0.6508; PRESS = 7.605E-004 and Adeq precision = 12.900

Table 11: ANOVA table for TRR (after backward elimination)

Sources	Sum of squares	df	Mean square	F-value	Prob>F	p value
Model	0.002	8	0.000	24.62	<0.0001	Significant
A-current	0.0015	1	0.001476056	147.7	<0.0001	
B-duty cycle (%)	3E-05	1	0.000032	3.203	0.0880	
C-powder concentration	9E-06	1	9.38889E-06	0.940	0.3434	
D-tool diameter	1E-05	1	0.0000125	1.251	0.2760	
AB	0.0001	1	0.00013225	13.24	0.0015	
AD	3E-05	1	0.00003025	3.027	0.0965	
CD	4E-05	1	0.00004225	4.228	0.0524	
C^2	0.0002	1	0.000233472	23.37	<0.0001	
Residual	0.0002	21	9.99206E-06	-	-	
Lack of fit	0.0002	16	1.13125E-05	1.962	0.2351	Non-significant
Pure error	3E-05	5	5.76667E-06	-	-	
Cor total	0.0022	29	-	-	-	

Std. Dev = 3.161E-003; R^2 = 0.9037; Mean = 0.030; Adj R^2 = 0.8670; C.V (%) = 10.54; Pred R^2 = 0.8109; PRESS = 4.119E - 004 and Adeq precision = 18.811

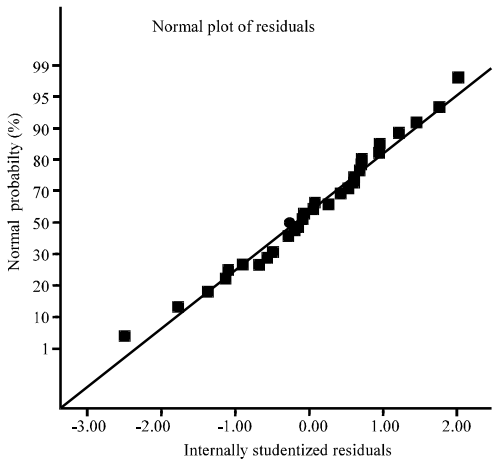

Fig. 7: Normal probability plot residuals for TWR

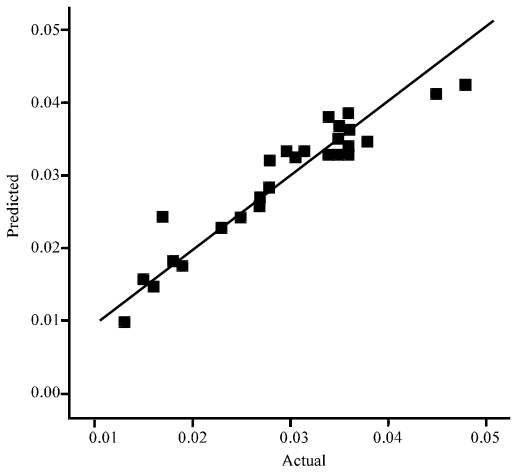

Fig. 8: Plot of actual vs. predicted response of TWR data

Final equation in terms of coded factors: TWR =+0.033+9.056E-003 A-1.333E-003 B-7.222E-004 C+8.333 E-004 D+2.875E-003 A B-1.375E-003 AD+1.625E - 003 CD -5.694E - 003 C^2. Final equation in terms of actual factors: TWR = +0.049500 -3.47222E - 003× Current -1.10648E -003× Duty cycle (%)+8.59028E -003× Powder concentration +4.27083 E - 004× Tool Diameter+1.59722 E -004× Current x Duty cycle (%) - 1.71875 E -004× Current

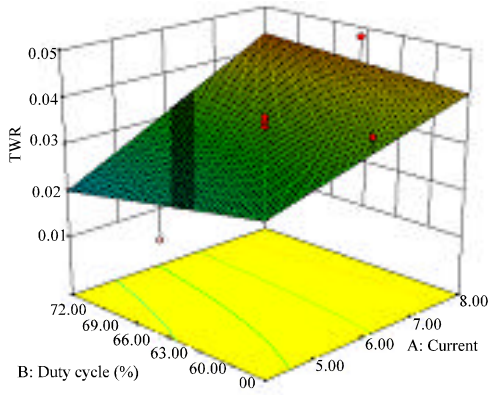

Fig. 9: Response surface for TWR showing effect of current and duty cycle

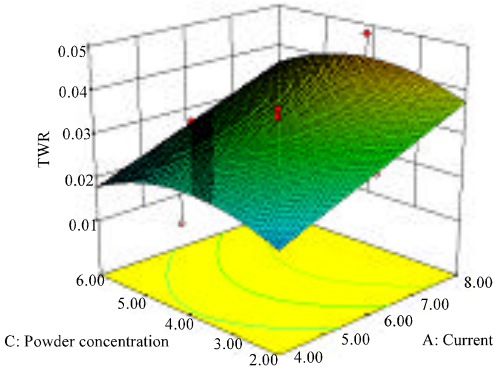

Fig. 10: Response surface for TWR showing effect of current and powder concentration

x Tool diameter+2.03125 E - 004× Powder concentration x Tool diameter - 1.42361 E - 003× Powder concentration^2. Figure 9-11 shows the estimated response surface for TWR in relation to the design parameters of peak current with tool diameter, powder concentration and duty cycle. As shown in Fig 9-11, the TWR tends to increase, considerably with increase in current for any value of other factors. Hence, maximum TWR is obtained at high current.

The TWR increases with increase in tool diameter owing to increase in current however tool diameter has not so, significant effect on TWR. TRR is found to increase with duty cycle. Long duty cycle results in less time for removal of gases produced and accumulated resulting in reduced TWR. Increase in powder concentration results in higher TWR but after certain level TWR starts reducing however, concentration has not so dominant effect on TWR.

Confirmation experiments: About 5 confirmation experiments have been conducted to check the validity of

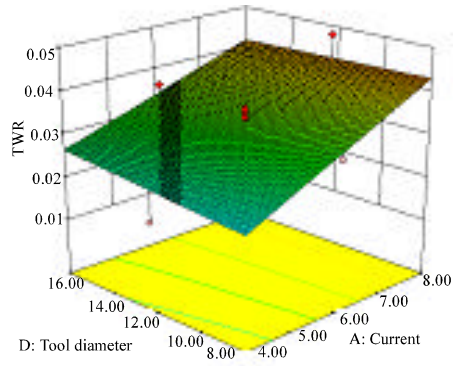

Fig. 11: Response surface for TWR showing effect of current and tool diameter

Table 12: Data for confirmation tests

Parameter settings				MRR			TWR		
Current	Duty cycle	Powder conc.	Tool diameter	Exp.	Pred.	Error	Exp.	Pred.	Error
6	54	4	12	6.26	5.99	4.31	0.033	0.035	-6.06
8	63	2	8	5.22	5.65	-8.23	0.040	0.039	2.50
6	72	4	16	4.79	4.94	-3.13	0.032	0.033	3.12
4	54	6	8	2.62	2.53	3.43	0.027	0.026	3.70
6	63	2	12	5.29	5.18	2.07	0.026	0.028	-7.69

developed models, results are shown in Table 12. It can be observed that the calculated error is small and tolerable. The error between experimental and predicted values for MRR and TWR are lie within±8.5%. This confirms excellent reproducibility of the experimental conclusions.

CONCLUSION

Micro nickel powder particles are mixed in EDM dielectric fluid. Empirical modeling with the help of RSM led to following conclusions:

- Current is most dominant factor affecting both MRR and TWR. Both the performance measures were observed an increasing trend with increase in current for any other settings of parameters
- MRR shows increasing trend for increase in powder concentration. The trend shows that MRR will increase further with further increase in concentration
- MRR increase with duty cycle but its effect is not so dominant
- Maximum MRR is observed for a tool diameter of 12 mm. MRR shows decreasing trend both below and above 12 mm tool diameter range
- Influences of tool diameter and duty cycle are not so dominant on TWR
- The confirmation tests showed that the error between experimental and predicted values of MRR and SR are within permissible range

REFERENCES

Chow, H.M., B.H. Yan, F.Y. Huang and J.C. Hung, 2000. Study of added powder in kerosene for the micro-slit machining of titanium alloy using electro-discharge machining. J. Mater. Proces. Technol., 101: 95-103.

Cogun, C., B. Ozerkan and T. Karacay, 2006. An experimental investigation on the effect of powder mixed dielectric on machining performance in electrical discharge machining. J. Eng. Manuf., 220: 1035-1050.

Erden, A. and S. Bilgin, 1980. Role of impurities in electric discharge machining. Proceedings of the 21st International Machine Tool Design and Research Conference, (IMTDRC'80), Macmillan, London, pp: 345-350.

Furutani, K. and K. Shiraki, 2002. Deposition of lubricant layer during finishing process by electrical discharge machining with molybdenum disulphide powder suspended in working fluid. Proceedings of JSME/ASME International Conference on Materials and Processing, (ICMP'02), Honolulu, Hawaii, USA., pp: 468-473.

Furutani, K., A. Saneto, H. Takezawa, N. Mohri and H. Miyake, 2001. Accertation of titanium carbide by electrical discharge machining with powder suspended in working fluid. Precision Eng., 25: 138-144.

Furutani, K., H. Sato and M. Suzuki, 2009. Influence of electrical conditions on performance of electrical discharge machining with powder suspended in working oil for titanium carbide deposition process. Int. J. Adv. Manuf. Technol., 40: 1093-1101.

Jeswani, M.L., 1981. Effects of the addition of graphite powder to kerosene used as the dielectric fluid in electrical discharge machining. Wear, 70: 133-139.

Kansal, H., S. Singh and P. Kumar, 2003. State of the art concerning powder mixed EDM. Proceedings of the International Conference on Emerging Technology, (ICET'03), KIIT, Bhubansewar, India.

Kansal, H.K., S. Singh and P. Kumar, 2005. Parametric optimization of powder mixed electrical discharge machining by response surface methodology. J. Mater. Proc. Technol., 169: 427-436.

Kansal, H.K., S. Singh and P. Kumar, 2007. Effect of silicon powder mixed EDM on machining rate of aisi D2 die steel. J. Manuf. Process., 9: 13-22.

Kobayashi, K., T. Magara, Y. Ozaki and T. Yatomi, 1992. The present and future developments of electrical discharge machining. Proceedings of the 2nd International Conference on Die and Mould Technology, (ICDMT'92), Singapore, pp: 35-47.

Kung, K.Y., J.T. Horng and K.T. Chiang, 2009. Material removal rate and electrode wear ratio study on the powder mixed electrical discharge machining of cobalt-bonded tungsten carbide. Int. J. Adv. Manuf. Technol., 40: 95-104.

Mohri, N., N. Saito, T. Takawashi and T. Takawashi, 1985. Mirror-like finishing by EDM. Proceedings of the 25th International Symposium on Machine Tool Design and Symposium, (ISMTDS'85), UK., pp: 329-336.

Mohri, N., J. Tsukamoto and M. Fujino, 1988. Surface modification by EDM-an innovation in EDM with semi-conductive electrodes. Proc. Winter Ann. Meet ASME, 34: 21-30.

Mohri, N., N. Saito, M. Higashi and N. Kinoshita, 1991. A new process of finish machining on free surface by EDM methods. CIRP Ann. Manuf. Technol., 40: 207-210.

Montgomery, D.C., 1997. Design and Analysis of Experiments. 4th Edn., John Wiley and Sons, New York, pp: 318-336.

Narumiya, H., N. Mohri, N. Saito, H. Otake, Y. Tsnekawa, T. Takawashi and K. Kobayashi, 1989. EDM by powder suspended working fluid. Proceedings of the 9th ISEM, (ISEM'89), Japan, pp: 5-8.

Okada, A., Y. Uno, K. Hirao and T. Takagi, 2000. Formation of hard layer by EDM with carbon powder mixed fluid using titanium electrode. Proceedings of 5th International Conference on Progress of Machining Technology, (ICPMT'00), USA., pp: 464-469.

Pecas, P. and E. Henriques, 2008a. Effect of the powder concentration and dielectric flow in the surface morphology in electrical discharge machining with powder-mixed dielectric (PMD-EDM). Int. J. Adv. Manuf. Technol., 37: 1120-1132.

Pecas, P. and E. Henriques, 2008b. Electrical discharge machining using simple and powder-mixed dielectric: The effect of the electrode area in the surface roughness and topography. J. Mater. Process. Technol., 200: 250-258.

Pecas, P. and E. Henriques, 2003. Influence of silicon powder-mixed dielectric on conventional electrical discharge machining. Int. J. Mach. Tools Manuf., 43: 1465-1471.

Prihandana, G.S., M. Mahardika, M. Hamdi, Y.S. Wong and K. Mitsui, 2009. Effect of micro-powder suspension and ultrasonic vibration of dielectric fluid in micro-EDM processes-Taguchi approach. Int. J. Machine Tools Manuf., 49: 1035-1041.

Simao, J., H.G. Lee, D.K. Aspinwall, R.C. Dewes and E.M. Aspinwall, 2003. Work piece surface modification using electrical discharge machining. Int. J. Machine Tools Manuf., 43: 121-128.

Tzeng, Y.F. and C.Y. Lee, 2001. Effects of powder characteristics on electro discharge machining efficiency. Int. J. Adv. Manuf. Technol., 17: 586-592.

Uno, Y. and A. Okada, 1997. Surface generation mechanism in electrical discharge machining with silicon powder mixed fluid. Int. J. Elec. Mach., 2: 13-18.

Uno, Y., A. Okada, Y. Hayashi and Y. Tabuchi, 1998. Surface integrity in EDM of aluminum bronze with nickel powder mixed fluid. J. Jpn. Soc. Elec. Mach. Eng., 32: 24-31.

Wong, Y.S., L.C. Lim, I. Rahuman and W.M. Tee, 1998. Near-mirror-finish phenomenon in EDM using powder-mixed dielectric. J. Mater. Process. Technol., 79: 30-40.

Wu, K.L., B.H. Yan, F.Y. Huang and S.C. Chen, 2005. Improvement of surface finish on SKD steel using electro-discharge machining with aluminum and surfactant added dielectric. Int. J. Machine Tools Manuf., 45: 1195-1201.

Yan, B.H. and S.L. Chen, 1993. Effects of dielectric with suspended aluminum powder on EDM. J. Chin. Soc. Mech. Eng., 14: 307-312.

Yan, B.H. and S.L. Chen, 1994a. Effect of ultrasonic vibration on electrical discharge machining characteristics of Ti-6Al-4V alloy. J. Jpn. Inst. Light Met., 44: 281-285.

Yan, B.H. and S.L. Chen, 1994b. Characteristics of SKD11 by complex process of electric discharge machining using liquid suspended with aluminum powder. J. Jpn. Inst. Light Met., 58: 1067-1072.

Yan, B.H., Y.C. Lin, F.Y. Huang and C.H. Wang, 2004. Surface modification of SKD 61 during EDM with metal powder in the dielectric. Mater. Trans., 42: 2597-2604.

Zhao, W.S., Q.G. Meng and Z.L. Wang, 2002. The application of research on powder mixed EDM in rough machining. J. Mater. Process. Technol., 129: 30-33.